

# Pulsed Rabi oscillations in quantum two-level systems: beyond the Area Theorem

Kevin A. Fischer,<sup>1,\*</sup> Lukas Hanschke,<sup>2</sup> Malte Kremser,<sup>2</sup> Jonathan J. Finley,<sup>2</sup> Kai Müller,<sup>2</sup> and Jelena Vučković<sup>1</sup>

<sup>1</sup>*E. L. Ginzton Laboratory, Stanford University, Stanford CA 94305, USA*

<sup>2</sup>*Walter Schottky Institut, Technische Universität München, 85748 Garching bei München, Germany*

(Dated: June 5, 2022)

The Area Theorem states that when a short optical pulse drives a quantum two-level system, it undergoes Rabi oscillations in the probability of scattering a single photon. In this work, we investigate the breakdown of the Area Theorem as both the pulse length becomes non-negligible and for certain pulse areas. Using simple quantum trajectories, we provide an analytic approximation to the photon emission dynamics of a two-level system. Our model provides an intuitive way to understand re-excitation, which elucidates the mechanism behind the two-photon emission events that can spoil single-photon emission. We experimentally measure the emission statistics from a semiconductor quantum dot, acting as a two-level system, and show good agreement with our simple model for short pulses. Additionally, the model clearly explains our recent results [K. Fischer and L. Hanschke, et al., *Nature Physics* (2017)] showing dominant two-photon emission from a two-level system for pulses with interaction areas equal to an even multiple of  $\pi$ .

## I. INTRODUCTION

One of the most fundamental building blocks of quantum optics is the single discrete atomic transition, which at its simplest is modeled as a quantum two-level system [1]. This type of system has been behind fundamental discoveries such as photon anti-bunching [2, 3], Mollow triplets [4, 5], and quantum interference of indistinguishable photons [6, 7]. After almost two decades of development in a solid-state environment, the quantum two-level system is now poised to serve the pivotal role of an on-demand single-photon source [2, 6, 8–16]—by converting laser pulses with Poissonian counting statistics to single photons—for quantum networks [17–19]. More recently, multi-photon quantum state generators have generated strong interest as replacements for the single-photon source in many quantum applications [20–22]. To this end, it was recently discovered that two-level systems may also generate pulses containing two-photons [23]. In this article, we show a simple intuitive model to better understand the temporal excitation dynamics of quantum two-level systems.

Consider an ideal two-level system [24], with a ground state  $|g\rangle$  and an excited state  $|e\rangle$ . Suppose the system is driven by an optical pulse, resonant with the  $|g\rangle \leftrightarrow |e\rangle$  transition and where the rotating wave approximation holds. As a function of the integrated pulse area

$$A(t) = \int_{-\infty}^t dt' \mu \cdot E(t')/\hbar, \quad (1)$$

where  $E(t')$  is the pulse's electric field and  $\mu$  the system's electric dipole moment, the system undergoes coherent oscillations between its ground  $|g\rangle$  and excited  $|e\rangle$  states. If the system is initially prepared in the ground state, the state after the system-pulse interaction is given by

$$|\psi_f(A)\rangle = \sqrt{1 - P_e(A(t))} |g\rangle + e^{-i\phi} \sqrt{P_e(A(t))} |e\rangle, \quad (2)$$

\* kevinf@stanford.edu

where  $\phi$  is a phase set by the laser field and  $P_e(A(t))$  is the area-dependent probability of exciting the two-level system. Examining  $P_e(A(t))$  shows Rabi oscillations that are perfectly sinusoidal

$$P_e(A(t)) = \sin^2(A(t)/2), \quad (3)$$

with the laser pulse capable of inducing an arbitrary number of rotations between  $|g\rangle$  and  $|e\rangle$ . After the system has interacted with the entire pulse, i.e. in the limit of  $t \rightarrow \infty$ , the probability of remaining in the excited state is

$$P_e(A(\infty)) = \sin^2(A(\infty)/2). \quad (4)$$

This statement is called the Area Theorem, in which Rabi oscillations occur as a function of the total interaction area of the pulse.

However, a realistic system is coupled to the outside world through its electric dipole and may spontaneously decay, which spoils the results of the Area Theorem [23, 25–27]. Previous works have shown its regime of validity occurs when the width of the pulse  $\tau_{\text{FWHM}}$  is very short compared to the spontaneous decay time  $\tau_e$ . That way, the system-pulse interaction occurs before any spontaneous emissions—we now explore this concept from a photon counting perspective [28]. First, suppose that no emission occurs during  $\tau_{\text{FWHM}}$ . Then, the probability that the system emits a single photon is given by  $P_e(A(\infty))$ , which is the final state occupation probability. But, suppose a single emission occurs during the system-pulse interaction. The probability density of the first emission occurring at time  $t_1$  can be understood simply as

$$f_1(A(t_1)) \approx \Gamma \sin^2(A(t_1)/2), \quad (5)$$

where  $\Gamma = 1/\tau_e$  is the rate of spontaneous emission. This density is inclusive in the sense that it counts trajectories both with one photon emission and with two photon emissions, because the emissions occur sequentially. The emission resets the system to its ground state, so

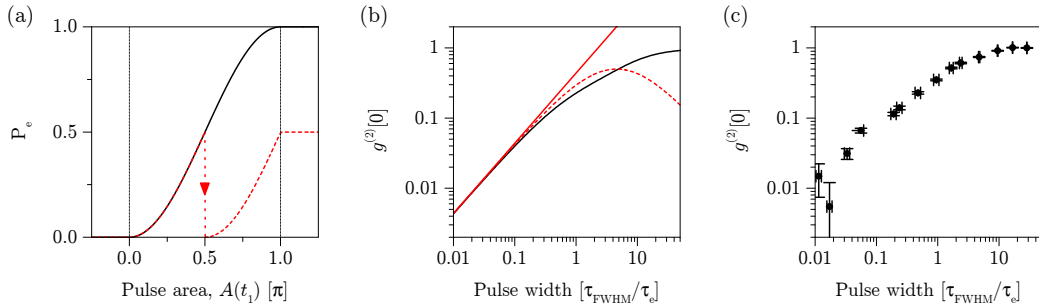


FIG. 1. Re-excitation dynamics for two-level system under interaction with a  $\pi$ -pulse, i.e.  $A(\infty) = \pi$ . (a) Two example quantum trajectories, with no photon emission (solid black) and one photon emission (dashed red) during the system-pulse interaction. Arrow indicates time of photon emission. (b) Measured degree of second-order coherence  $g^{(2)}[0]$  under excitation by a Gaussian pulse, simulated with the quantum regression theorem (black) and estimated from our simple analytic approach—linear estimate (solid red) and polynomial estimate (dashed red). (c) Experimentally measured degree of second-order coherence, obtained when resonantly exciting a two-level system made up of excitonic states from a deterministically charged quantum dot.

the conditional probability of the second emission (after the system-pulse interaction) is then given roughly by the remaining excited-state occupation  $P_e(A(\infty) - A(t))$ . Thus, the probability density for two emissions to occur, with one occurring during the system-pulse interaction and the second afterwards, is given by

$$p_2(A(t_1); A(\infty)) \approx f_1(A(t_1)) P_e(A(\infty) - A(t_1)). \quad (6)$$

The total probability for two emissions is then given by exploring all possible ways for the first emission to occur during the system-pulse interaction, so

$$P_2 = \int dt_1 p_2(A(t_1); A(\infty)). \quad (7)$$

This confirms the heuristic that  $P_2$  is of order  $\tau_{\text{FWHM}}/\tau_e$  for non-trivial pulse areas. By extension, the probability of  $n$  emissions is of order  $(\tau_{\text{FWHM}}/\tau_e)^{n-1}$ . We further discuss the case of our analytic model for three emissions in Appendix A, but ignore the possibility of  $n > 2$  emissions for our analytic model in the main text. We note that this is valid for short pulses, but when  $\tau_{\text{FWHM}} \approx \tau_e$  multi-photon emission sequences begin to dominate and our model no longer holds.

## II. BREAKDOWN WITH INCREASING PULSE LENGTH

Although remarkably simple, our trajectory formalism allows for analytic exploration of an important phenomenon in solid-state single-photon sources—many single-photon sources behave as nearly ideal quantum two-level systems [9, 29, 30]. These systems operate by sending a short pulse of area  $A(\infty) = \pi$  to excite the system to  $|e\rangle$  with almost unity probability, which results in emission of a single-photon wavepacket with high probability [31]. The target single-photon wavepackets may be used in quantum information systems in the future, however, some of these systems have extremely stringent

requirements against multiphoton errors [32, 33]. Thus, our proposed model for understanding multiphoton errors, as due to re-excitation in a two-level system, can be used to help identify useful regimes of operation.

To explore this concept further, we suppose the excitation of a two-level system by a short pulse of area  $A(\infty) = \pi$ . The dynamics of this process as a function of interacted pulse area are depicted in Fig. 1a. A standard quantum trajectory [28] with no re-excitation is shown as the black curve, where the single-photon emission would occur some time long after the system-pulse interaction. Because the  $n$ -photon generation probability scales as  $(\tau_{\text{FWHM}}/\tau_e)^{n-1}$ , we only need to consider the error due to a single re-excitation. The red dashed curve depicts a trajectory with an emission occurring after  $A(t_1) = \pi/2$  has been interacted. Similar to the trajectory with a single emission, the re-excited system is most likely to emit its second photon long after the system-pulse interaction has occurred.

By integrating over all possible trajectories, we can compute the error rate  $P_2(\tau_{\text{FWHM}}; A(\infty) = \pi)$ , which was only extracted experimentally [27] and numerically [31] thus far. This can then be used to estimate the experimentally measurable metric of the quality of a single-photon source [31], the degree of second-order coherence

$$g^{(2)}[0] = \frac{\sum_k k(k-1)P_k}{(\sum_k kP_k)^2}. \quad (8)$$

As the pulse-width decreases  $g^{(2)}[0]$  approaches from  $1 \rightarrow 0$ , shown as the black curve in Fig. 1b (computed as in reference [31]), indicating an increase in the quality of the single-photon nature of the wavepacket. For short pulses, the system acts as a good single-photon source and  $g^{(2)}[0] \approx 2P_2$ , which we can calculate from our analytical expression (solid red line). Although any ideal Rabi oscillation of equivalent  $A(\infty)$  is isomorphic by a nonlinear coordinate transformation in time, the precise form of the pulse can change  $P_2$  for a given  $\tau_{\text{FWHM}}$  due to integration over the time variable. For example, a Gaussian pulse yields  $P_2 = 0.2188\tau_{\text{FWHM}}/\tau_e$  while a square

pulse yields  $P_2 = 0.125\tau_{\text{FWHM}}/\tau_e$ . (We note here that we considered an incident Gaussian pulse where  $\tau_{\text{FWHM}}$  is the width in energy, by convention in the field of single-photon sources.)

However, we can obtain an even better analytic approximation by considering that as  $P_2$  increases while  $A(\infty) = \pi$ ,  $P_1$  must decrease to conserve probability. Therefore

$$g^{(2)}[0] \approx \frac{2P_2}{(1+P_2)^2}, \quad (9)$$

which is plotted as the dashed red curve. This approximation works quite well until  $\tau_{\text{FWHM}} \approx \tau_e$ , where the analytic model does not correctly capture the saturation behavior of the second-order coherence. For long pulse lengths, the statistics tend towards Poissonian due to the possibility of many randomly distributed photon emissions occurring.

To verify that our simple model has real predictive power for short pulses, we experimentally measured the degree of second-order coherence  $g^{(2)}[0]$  of pulses scattered by a resonantly driven two-level system (Fig. 1c). We explored a much broader range of pulse widths compared to previous data, showing a complete series from a few ps to 10's of ns, which allows us to explore how our analytic model deviates from experiment for long pulses as well. Our two-level system of choice was the single electron to trion transition of a charged InAs/GaAs quantum dot (see Supplementary material for data and details on the experiments). Good agreement can be seen between the full quantum-optical model and data, with only small differences that result from experimental inaccuracies (see Supplementary material). Meanwhile, the analytic model gives good agreement until  $\tau_{\text{FWHM}} \approx \tau_e$ .

In summary, we have quantified how the Area Theorem breaks down as a function of pulse length. This discussion can provide an important limit on the achievable source error rates for a given ratio of pulse length to spontaneous emission lifetime, an important addition to previous studies on the phonon-induced limitations for emission of indistinguishable photons from solid-state devices [34–37]. We expect new directions in research on solid-state sources to involve understanding the interplay of pulsed excitation with phonon dynamics [38–40]. For short pulses, we believe the phonon dynamics work to incoherently populate (or re-excite) the system: most likely with the same type of linear dependence as the coherent excitation mechanism we have identified [23].

### III. BREAKDOWN FOR EVEN PI AREAS

As recently discovered [23], the Area Theorem breaks down when  $A(\infty) = 2m\pi$  and  $m \in \{1, 2, 3, \dots\}$ . We now explore this point with our simple model. To help understand this breakdown, we introduce a new probability

density

$$p_1(A(t_1)) \approx f_1(A(t_1)) - p_2(A(t_1); A(\infty)) \quad (10)$$

$$= f_1(A(t_1)) (1 - P_e(A(\infty) - A(t_1))), \quad (11)$$

which represents the exclusive probability density for a single photon emission during the system-pulse interaction, i.e. emission of one photon during interaction time and no emission later.

First, consider the probability densities for a  $\pi$  pulse (Fig. 2a). The trajectory if no photon emission occurs is again shown as a function of interacted pulse area; however, we now additionally show  $p_1(A(t_1))$  and  $p_2(A(t_1); A(\infty))$ . Integrals of the densities give the probabilities for one or two photon emissions to occur, respectively, with the only or first emission to occur during the system-pulse interaction time. The shaded regions hence depict total probabilities for exclusive types of emission events. By considering the fully time-resolved probability density for two photon emissions  $p_2(A(t_1), t_2)$ , we can also clarify the precise meaning of the second emission occurring within the spontaneous emission lifetime. Specifically,  $p_2(A(t_1), t_2)$  is approximately separable as  $p_2(A(t_1), t_2) \approx p_2(A(t_1); A(\infty)) e^{-t_2/\tau_e}$ , which is plotted for a  $\pi$  pulse in (Fig. 2e). Additionally, consider two other scenarios.

1. The situation is dramatically different when the pulse is long compared to the emission lifetime and multiple re-excitation events can occur (see Appendix B).
2. The results for  $A(\infty) = \pi$  are similar to all pulses with odd- $\pi$  areas. For example, examine the densities for  $\pi$  (Fig. 2a,e) and  $3\pi$  (Fig. 2c,g) pulse areas: they are comparable whereby the densities from  $A(\infty) = \pi$  have been tessellated three times for  $A(\infty) = 3\pi$ .

On the other hand, the situation for  $p_1(A(t_1))$  is radically different for a  $2\pi$  pulse (Fig. 2b,f). Importantly, the Area Theorem requires the excited-state population to return to zero after the system-pulse interaction, as shown by the dashed black line. Hence, we can use our single-photon emission density that was defined *only during the system-pulse interaction* to compute  $P_1$  as  $P_1 = \int dt_1 p_1(A(t_1))$ , which gives the result that both  $P_2$  and  $P_1$  are of order  $\tau_{\text{FWHM}}/\tau_e$ . This procedure yields  $P_2/P_1 \approx 2.33$  for a Gaussian pulse and  $P_2/P_1 = 3$  for a square pulse, with the remarkable result that  $P_2 > P_1$ . Interestingly,  $P_2$  is emphasized because the most likely initial emission occurs when roughly  $\pi$  of the area has been absorbed, forcing a re-excitation with almost unity probability by the remaining  $\pi$  area. In fact, this result is nearly identical for all pulses of even- $\pi$  area (see Fig. 2d,h for  $A(\infty) = 4\pi$ , where the probability densities for  $A(\infty) = 2\pi$  have just been copied a second time). Nearly constant ratios of  $P_2/P_1$  for all even- $\pi$  areas occur because both  $p_1(A(t_1))$  and  $p_2(A(t_1); A(\infty))$  are periodic with area  $2\pi$ . The most important consequence of the periodicity is that  $P_2 > P_1$  for even arbitrarily short pulses,

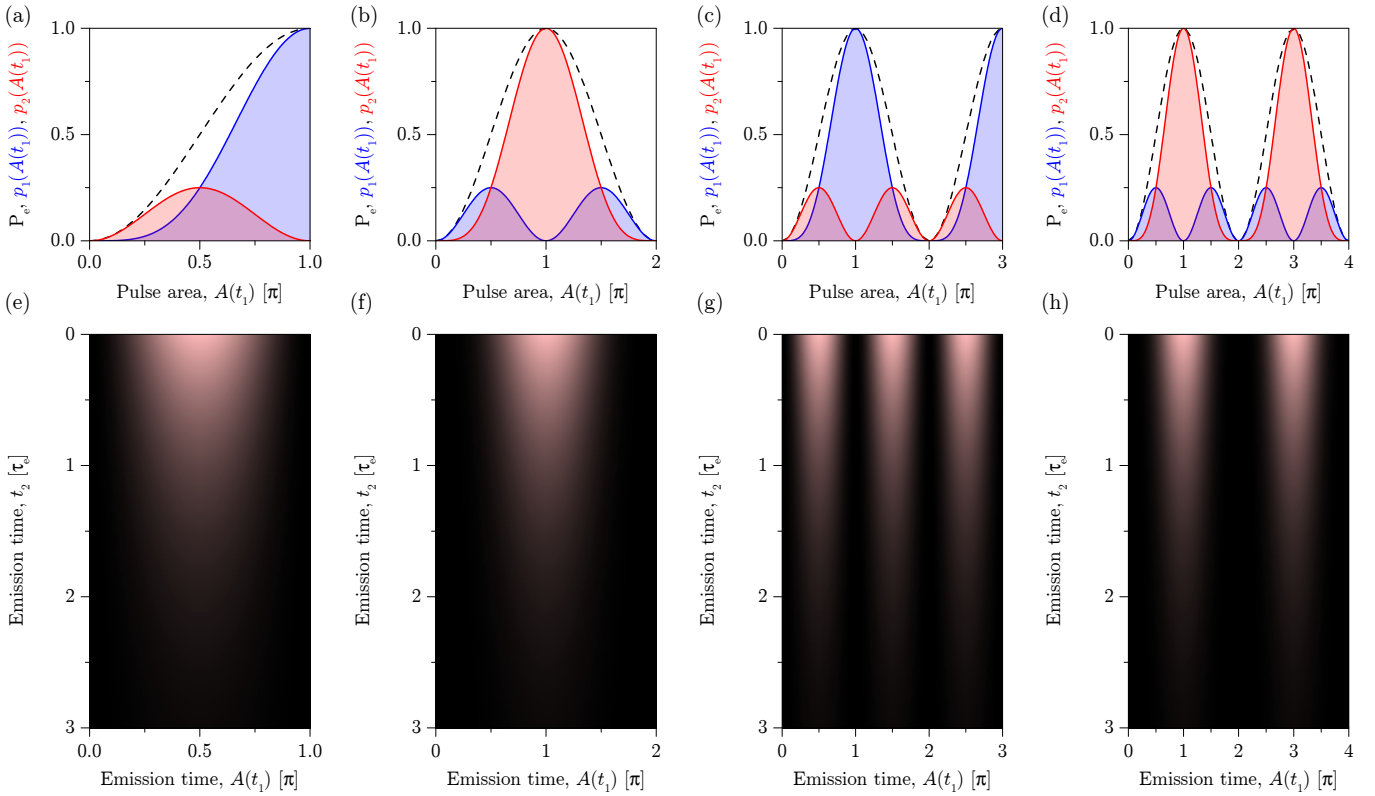


FIG. 2. Re-excitation dynamics for a two-level system under interaction with  $m\pi$ -pulses, i.e.  $A(\infty) = m\pi$  for  $m \in \{1, 2, 3, 4\}$ . (a)-(d) Probability of system being in the excited state  $P_e$  if no emissions occur, and probability density  $p_1(A(t_1))$  for a single photon emission at time  $t_1$  and  $p_2(A(t_1); A(\infty))$  for a pair of photon emissions to begin at time  $t_1$ . (e)-(h) Fully time-resolved probability density  $p_2(A(t_1), t_2)$  for a pair of photon emissions, assuming the system-pulse interaction time is very short compared to the excited state lifetime, i.e.  $\tau_{\text{FWHM}} \ll \tau_e$ .

showing a dramatic result in the breakdown of the Area Theorem when  $A(\infty) = 2m\pi$ .

#### IV. COMPARISON TO REALISTIC RABI OSCILLATIONS

In the final section, we compare the results generated with our simple model to those from a full quantum mechanical simulation [23, 31]. Here, we take a typical Gaussian pulse of length  $\tau_{\text{FWHM}} = 0.1\tau_e$  and look at the Rabi oscillations (Fig. 3a) and photon statistics (Fig. 3b) versus interacted pulse area. First for a reference, consider the ideal probabilities to scatter a single photon  $P_1$  if spontaneous emission is ignored—these are the well-known sinusoidal Rabi oscillations predicted by the Area Theorem (solid black curve). When the effects of spontaneous emission are included, re-excitation causes  $P_2$  to become non-negligible (red). Values of  $P_2$  can be accurately computed for any pulse area using our model (solid red curve), as compared to the full quantum mechanical calculation (red crosses). Meanwhile,  $P_1$  as derived from the full quantum mechanical simulation deviates from perfect sinusoidal behavior (blue crosses). Nevertheless, its values can be accurately extracted from our simple

model at the significant points of  $A(\infty) = m\pi$  (blue points). For even integers of  $m$ ,  $P_1 = \int dt_1 p_1(A(t_1))$ , and for odd integers of  $m$ ,  $P_1 = 1 - P_2$ .

We can also consider the photon statistics of the emission  $g^{(2)}[0]$  and the variance of the emission relative to the variance of a coherent state

$$\text{Var}[n] = \frac{\sum_k (k^2 - (\text{E}[n])^2) P_k}{k}. \quad (12)$$

The relative photon-number variance is lowest around odd multiples of  $\pi$ , indicating the emission of a highly pure single-photon state. Around even-multiples of  $\pi$ , however, the emission is highly super-Poissonian because two-photon emission is emphasized, i.e.  $P_2 \gg P_1$ . Thus the second-order coherence bunches,  $g^{(2)}[0] > 1$ , and the relative photon number variance peaks. All of these important points at  $A(\infty) = m\pi$  can accurately be estimated from our simple model, plotted as the black and purple points, which agree very well with the full simulated values. This agreement furthers our assertion that the probability of three emissions  $P_3$  is negligible because it is of order  $(\tau_{\text{FWHM}}/\tau_e)^2$ . From our discussion, we clearly see the Area Theorem alone is incapable of correctly capturing the dynamics and photon statistics around  $A(\infty) = 2m\pi$ . The failure holds even for arbi-

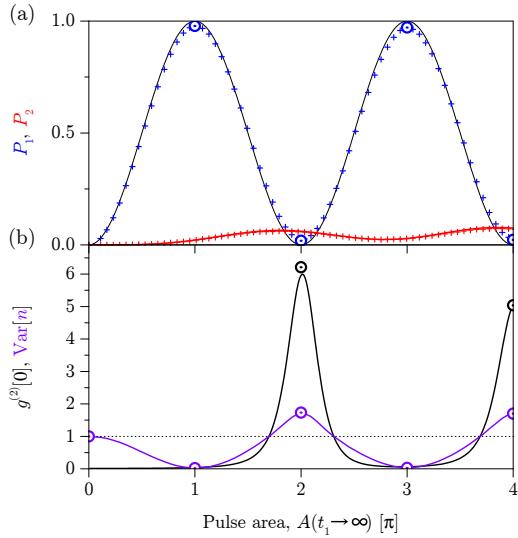


FIG. 3. Photon emission statistics of a two-level system under excitation by a Gaussian pulse of  $\tau_{\text{FWHM}} = 0.1\tau_e$ . (a) Probabilities for  $P_1$  single and  $P_2$  pairs of photon emissions. Black curve shows  $P_1$  for an ideal Rabi oscillation, while crosses indicate simulated values using a full quantum trajectory calculation that includes spontaneous emission. Red curve and blue points show estimates based on our simple analytic approach. (b) Exact simulations for the variance relative to a coherent state  $\text{Var}[n]$  and for  $g^{(2)}[0]$  as curves, while black and purple points show estimates based on our simple analytic approach. Dotted black line shows coherence statistics of the incident laser pulse.

trarily short pulse areas, where the second-order coherence diverges resulting in a singularity.

## ACKNOWLEDGMENTS

We gratefully acknowledge financial support from the National Science Foundation (Division of Materials Research - Grant. No. 1503759) and the Bavaria California Technology Center (BaCaTeC). KAF acknowledges support from the Lu Stanford Graduate Fellowship and the National Defense Science and Engineering Graduate Fellowship. KM acknowledges support from the Bavarian Academy of Sciences and Humanities.

## APPENDIX A: THREE-PHOTON EMISSION PROBABILITY DENSITY

In this appendix, we explore the possibility for three photoemissions to occur during drive by a short pulse. This scenario with three emissions requires two emissions to occur during the pulse width  $\tau_{\text{FWHM}}$ , and hence the total probability for three emissions  $P_3$  is of the order  $(\tau_{\text{FWHM}}/\tau_e)^2$ . To arrive at the estimate for  $P_3$ , we begin by imagining a trajectory that has two emissions during the pulse length. The first emission occurs with density

$f_1(A(t_1))$  and the second emission occurs with density  $f_1(A(t_2) - A(t_1))$ , where the expression holds for  $t_2 > t_1$ . When  $\tau_{\text{FWHM}}/\tau_e$  is small, the final emission is most likely to occur with the final occupation probability of the excited state  $P_e(A(\infty) - A(t_1) - A(t_2))$ . Thus, the probability density for three emissions to occur is given

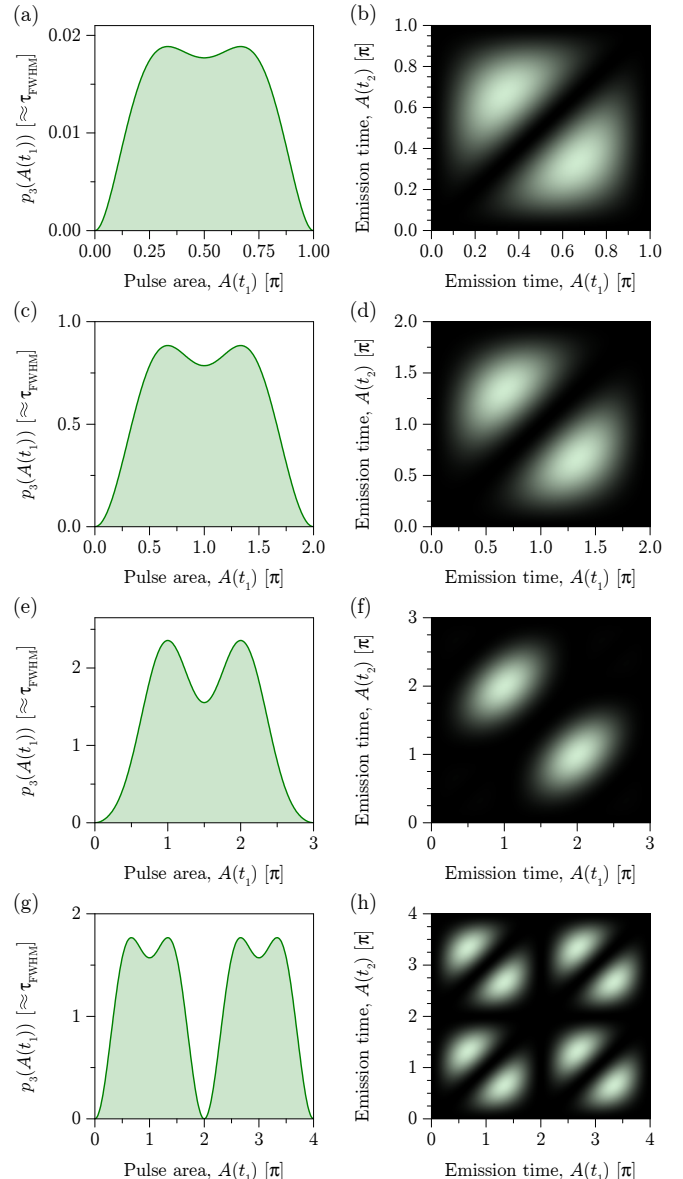


FIG. 4. Three-photon emission dynamics for two-level system under interaction with  $m\pi$ -pulses, i.e.  $A(\infty) = m\pi$  for  $m \in \{1, 2, 3, 4\}$ . (a,c,e,g) Three-photon emission probability density  $p_3(A(t_1))$  at time  $t_1$ , i.e. all the ways three-photon emission might contribute to  $E[n(t)]$ . Note,  $p_3(A(t_1))$  is not dimensionless. (b,d,f,h) Three-photon emission probability density  $p_3(A(t_1), A(t_2))$ —along the third time axis  $t_3$ , the probability density  $p_3$  decays exponentially like  $p_2$  does along  $t_2$ .

by

$$p_3(A(t_1), A(t_2), t_3) \approx f_1(A(t_1)) f_1(A(t_2) - A(t_1)) \cdot P_e(A(\infty) - A(t_1) - A(t_2)) e^{-t_3/\tau_e} \quad (13)$$

for  $t_2 > t_1$ . Because we do not care if the first detection was at time  $t_1$  or  $t_2$ , the probability density is symmetric with exchange of these time indices. We can, of course, obtain the marginal probability densities

$$p_3(A(t_1), A(t_2)) = \int dt_3 p_3(A(t_1), A(t_2), t_3), \quad (14)$$

which inherits the symmetry of  $p_3(A(t_1), A(t_2), t_3)$ , and

$$p_3(A(t_1)) = \int dt_2 p_3(A(t_1), A(t_2)). \quad (15)$$

Using these densities, we explore a number of points. Along the third detection time axis  $t_3$ , the probability density decays exponentially and is rather uninteresting. The remaining densities have interesting behavior; consider  $p_3(A(t_1), A(t_2))$  as plotted in Fig. 4b,d,f,h for  $A(\infty) = m\pi$  and  $m \in \{1, 2, 3, 4\}$ . These densities are almost all identical in shape for  $m \in \{1, 2, 3\}$ . The similarity of the shape owes to the fact that until the interaction area is greater than  $3\pi$ , the optimal way to achieve a three-photon emission is to divide the pulse into thirds—the increase in excitation probability is then monotonically increasing between emissions. This division is reflected in the two bright regions of the densities, which correlate emissions around  $A(\infty)/3$  to those around  $2A(\infty)/3$ . Meanwhile for  $4\pi$ , enough area is present that the optimum division must include Rabi flopping between the ground and excited states, resulting in an increase in the number of optimal ways to achieve three-photon emission.

Next, consider the densities  $p_3(A(t_1))$  as plotted in Fig. 4a,c,e,g for  $A(\infty) = m\pi$  and  $m \in \{1, 2, 3, 4\}$ . These densities can easily be understood as all possible ways to achieve a photon emission after  $A(t_1)$  has been absorbed, out of emission events involving three photoemissions. Their integrals yield  $P_3$  and are depicted as the shaded regions. Notably,  $P_3$  is almost two orders of magnitude lower for  $A(\infty) = \pi$ , which occurs because not enough interaction area is yet present to significantly excite the system between any of the photon emissions, i.e.  $\sin^2((2\pi/3)/2)^3 \gg \sin^2((\pi/3)/2)^3$ . As a final remark, we note the connection between photon flux and probability

densities. Generally, as long as the marginal densities for photoemission  $p_n(t)$  are constructed as exclusive events, then

$$\Gamma E[n(t)] = \sum_n p_n(t), \quad (16)$$

which represents all possible ways to achieve a photon emission at time  $t_1$ .

## APPENDIX B: SECOND-ORDER COHERENCE WHEN DRIVEN BY A LONG PULSE

In this appendix, we consider the second-order coherence of the emission from a two-level system when it is driven by a long pulse ( $\tau_{FWHM} \gg \tau_e$ ) with  $\pi$  area. For short pulses, the second-order coherence is given by  $G^{(2)}(t_1, t_2) = 2p_2(A(t_1), t_2)$  for  $t_2 > t_1$ . Because we do not care if the first detection was at time  $t_1$  or  $t_2$ ,  $G^{(2)}(t_1, t_2)$  is symmetric with exchange of these time indices. Thus, short pulses yield two thin slivers of second-order coherence that have dimensions  $\tau_{FWHM} \times \tau_e$  and  $\tau_e \times \tau_{FWHM}$ . However, for long pulses  $G^{(2)}(t_1, t_2)$  is an inclusive moment of the probability densities rather than exclusive. In this scenario, multiphoton emissions also contribute to  $G^{(2)}(t_1, t_2)$  giving a giant blob of second-order coherence (Fig. 5). The blob has zero values for the equal time correlations  $G^{(2)}(t_1, t_1)$  since the two-level system only can emit one photon at a time. Notably, when the pulse is long it inherits the coherence of the incident laser beam and  $g^{(2)}[0] = 1$ .

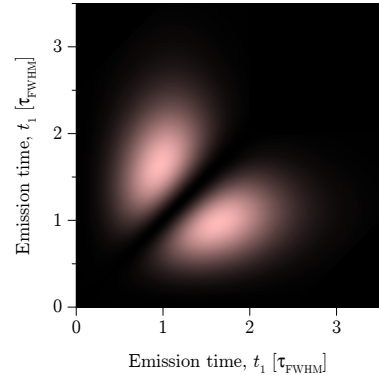


FIG. 5. Second-order coherence  $G^{(2)}(t_1, t_2)$  of emission from a two-level system under excitation by a long pulse ( $\tau_{FWHM} = 3.3\tau_e$ ) with area  $A(\infty) = \pi$ .

---

[1] C. Cohen-Tannoudji, J. Dupont-Roc, G. Grynberg, and P. Thickstun, *Atom-photon interactions: basic processes and applications* (Wiley Online Library, 1992).  
[2] P. Michler, A. Kiraz, C. Becher, W. V. Schoenfeld, P. M. Petroff, L. Zhang, E. Hu, and A. Imamoglu, *A quant-*

*tum dot single-photon turnstile device*, *Science* **290**, 2282 (2000).  
[3] H. J. Kimble, M. Dagenais, and L. Mandel, *Photon antibunching in resonance fluorescence*, *Phys. Rev. Lett.* **39**, 691 (1977).

[4] E. B. Flagg, A. Muller, J. W. Robertson, S. Founta, D. G. Deppe, M. Xiao, W. Ma, G. J. Salamo, and C. K. Shih, *Resonantly driven coherent oscillations in a solid-state quantum emitter*, *Nat. Phys.* **5**, 203 (2009).

[5] B. R. Mollow, *Power spectrum of light scattered by Two-Level systems*, *Phys. Rev.* **188**, 1969 (1969).

[6] C. Santori, D. Fattal, J. Vučković, G. S. Solomon, and Y. Yamamoto, *Indistinguishable photons from a single-photon device*, *Nature* **419**, 594 (2002).

[7] C. K. Hong, Z. Y. Ou, and L. Mandel, *Measurement of subpicosecond time intervals between two photons by interference*, *Phys. Rev. Lett.* **59**, 2044 (1987).

[8] Y.-M. He, Y. He, Y.-J. Wei, D. Wu, M. Atatüre, C. Schneider, S. Höfling, M. Kamp, C.-Y. Lu, and J.-W. Pan, *On-demand semiconductor single-photon source with near-unity indistinguishability*, *Nat. Nano.* **8**, 213 (2013).

[9] C. Schneider, P. Gold, C.-Y. Lu, S. Höfling, J.-W. Pan, and M. Kamp, in *Engineering the Atom-Photon Interaction* (Springer, 2015) pp. 343–361.

[10] Z. Yuan, B. E. Kardynal, R. M. Stevenson, A. J. Shields, C. J. Lobo, K. Cooper, N. S. Beattie, D. A. Ritchie, and M. Pepper, *Electrically driven single-photon source*, *Science* **295**, 102 (2002).

[11] J. Claudon, J. Bleuse, N. S. Malik, M. Bazin, P. Jaffrennou, N. Gregersen, C. Sauvan, P. Lalanne, and J.-M. Gérard, *A highly efficient single-photon source based on a quantum dot in a photonic nanowire*, *Nat. Photon.* **4**, 174 (2010).

[12] S. Unsleber, Y.-M. He, S. Gerhardt, S. Maier, C.-Y. Lu, J.-W. Pan, N. Gregersen, M. Kamp, C. Schneider, and S. Höfling, *Highly indistinguishable on-demand resonance fluorescence photons from a deterministic quantum dot micropillar device with 74% extraction efficiency*, *Opt. express* **24**, 8539 (2016).

[13] A. Schleehahn, A. Thoma, P. Munnelly, M. Kamp, S. Höfling, T. Heindel, C. Schneider, and S. Reitzenstein, *An electrically driven cavity-enhanced source of indistinguishable photons with 61% overall efficiency*, *APL Photonics* **1**, 011301 (2016).

[14] N. Somaschi, V. Giesz, L. De Santis, J. Loredo, M. Almeida, G. Hornecker, S. Portalupi, T. Grange, C. Antón, J. Demory, et al., *Near-optimal single-photon sources in the solid state*, *Nat. Photon.* **10**, 340 (2016).

[15] X. Ding, Y. He, Z.-C. Duan, N. Gregersen, M.-C. Chen, S. Unsleber, S. Maier, C. Schneider, M. Kamp, S. Höfling, et al., *On-demand single photons with high extraction efficiency and near-unity indistinguishability from a resonantly driven quantum dot in a micropillar*, *Phys. Rev. Lett.* **116**, 020401 (2016).

[16] P. Michler, ed., *Quantum Dots for Quantum Information Technologies* (Springer, 2017).

[17] J. C. Loredo, M. A. Broome, P. Hilaire, O. Gazzano, I. Sagnes, A. Lemaitre, M. P. Almeida, P. Senellart, and A. G. White, *BosonSampling with single-photon fock states from a bright solid-state source*, (2016), arXiv:arXiv:1603.00054 [quant-ph].

[18] I. Aharonovich, D. Englund, and M. Toth, *Solid-state single-photon emitters*, *Nat. Photon.* **10**, 631 (2016).

[19] J. L. O'Brien, A. Furusawa, and J. Vučković, *Photonic quantum technologies*, *Nat. Photon.* **3**, 687 (2009).

[20] A. Rundquist, M. Bajcsy, A. Majumdar, T. Sarmiento, K. Fischer, K. G. Lagoudakis, S. Buckley, A. Y. Piggott, and J. Vučković, *Nonclassical higher-order photon correlations with a quantum dot strongly coupled to a photonic-crystal nanocavity*, *Phys. Rev. A* **90**, 023846 (2014).

[21] C. S. Muñoz, E. Del Valle, A. G. Tudela, K. Müller, S. Lichtmannecker, M. Kaniber, C. Tejedor, J. Finley, and F. Laussy, *Emitters of n-photon bundles*, *Nat. Photon.* **8**, 550 (2014).

[22] I. Afek, O. Ambar, and Y. Silberberg, *High-noon states by mixing quantum and classical light*, *Science* **328**, 879 (2010).

[23] K. A. Fischer, L. Hanschke, J. Wierzbowski, T. Simmet, C. Dory, J. J. Finley, J. Vučković, and K. Müller, *Signatures of two-photon pulses from a quantum two-level system*, *Nat. Phys.* (2017).

[24] B. W. Shore, *Manipulating quantum structures using laser pulses* (Cambridge University Press, Cambridge, 2011).

[25] P. A. Rodgers and S. Swain, *Time-dependent pulses in quantum optics: the use of light's perturbation theory*, *J. Phys. B At. Mol. Opt. Phys.* **20**, 617 (1987).

[26] J. Zakrzewski, K. Rzazewski, and M. Lewenstein, *Theory of fluorescence spectra induced by short laser pulses*, *J. Opt. Soc. Am. B* **3**, 22 (1986).

[27] A. C. Dada, T. S. Santana, R. N. Malein, A. Koutroumanis, Y. Ma, J. M. Zajac, J. Y. Lim, J. D. Song, and B. D. Gerardot, *Indistinguishable single photons with flexible electronic triggering*, *Optica* **3**, 493 (2016).

[28] H. Carmichael, *An open systems approach to quantum optics: lectures presented at the Université Libre de Bruxelles, October 28 to November 4, 1991*, Vol. 18 (Springer Science & Business Media, 2009).

[29] H. Wang, Z.-C. Duan, Y.-H. Li, S. Chen, J.-P. Li, Y.-M. He, M.-C. Chen, Y. He, X. Ding, C.-Z. Peng, C. Schneider, M. Kamp, S. Höfling, C.-Y. Lu, and J.-W. Pan, *Near-Transform-Limited single photons from an efficient Solid-State quantum emitter*, *Phys. Rev. Lett.* **116**, 213601 (2016).

[30] A. V. Kuhlmann, J. H. Prechtel, J. Houel, A. Ludwig, D. Reuter, A. D. Wieck, and R. J. Warburton, *Transform-limited single photons from a single quantum dot*, *Nat. Commun.* **6**, 8204 (2015).

[31] K. A. Fischer, K. Müller, K. G. Lagoudakis, and J. Vučković, *Dynamical modeling of pulsed two-photon interference*, *New J. Phys.* **18**, 113053 (2016).

[32] K. Azuma, K. Tamaki, and H.-K. Lo, *All-photonic quantum repeaters*, *Nat. Commun.* **6** (2015).

[33] P. Kok, W. J. Munro, K. Nemoto, T. C. Ralph, J. P. Dowling, and G. J. Milburn, *Linear optical quantum computing with photonic qubits*, *Rev. Mod. Phys.* **79**, 135 (2007).

[34] J. Iles-Smith, D. P. McCutcheon, A. Nazir, and J. Mørk, *Phonon scattering inhibits simultaneous near-unity efficiency and indistinguishability in semiconductor single-photon sources*, *Nat. Photon.* (2017).

[35] P. Kaer, P. Lodahl, A.-P. Jauho, and J. Mørk, *Microscopic theory of indistinguishable single-photon emission from a quantum dot coupled to a cavity: The role of non-markovian phonon-induced decoherence*, *Phys. Rev. B* **87**, 081308 (2013).

[36] P. Kaer, N. Gregersen, and J. Mørk, *The role of phonon scattering in the indistinguishability of photons emitted from semiconductor cavity qed systems*, *New J. Phys.* **15**, 035027 (2013).

[37] A. Thoma, P. Schnauber, M. Gschrey, M. Seifried, J. Wolters, J.-H. Schulze, A. Strittmatter, S. Rodt,

A. Carmele, A. Knorr, *et al.*, *Exploring dephasing of a solid-state quantum emitter via time-and temperature-dependent hong-ou-mandel experiments*, Phys. Rev. Lett. **116**, 033601 (2016).

[38] C. Gustin and S. Hughes, *Influence of electron-phonon scattering for an on-demand quantum dot single-photon source using cavity-assisted adiabatic passage*, arXiv preprint arXiv:1706.07521 (2017).

[39] K. Müller, K. A. Fischer, C. Dory, T. Sarmiento, K. G. Lagoudakis, A. Rundquist, Y. A. Kelaita, and J. Vučković, *Self-homodyne-enabled generation of indistinguishable photons*, Optica **3**, 931 (2016).

[40] K. Müller, K. A. Fischer, A. Rundquist, C. Dory, K. G. Lagoudakis, T. Sarmiento, Y. A. Kelaita, V. Borish, and J. Vučković, *Ultrafast polariton-phonon dynamics of strongly coupled quantum dot-nanocavity systems*, Phys. Rev. X **5**, 031006 (2015).